Ion-motion effect in the Stark profiles of Hα and Hβ

C. Fleurier, G. Coulaud, and P. Ranson
Centre de Recherche sur la Physique des Hautes Températures, Centre National de la Recherche Scientifique, 45045 Orléans Cédex, France

J. Chapelle
Unité d'Enseignement et de Recherches de Sciences Fondamentales et Appliquées, Université d'Orléans, 45045 Orléans Cédex, France
(Received 11 June 1979)

The effects of ion motion on the Stark profiles of the lines Hα and Hβ have been studied in a plasma jet for an electron density range from 10^{15} cm^{-3} up to 2×10^{16} cm^{-3}. The ion velocity was changed in the ratio 0.5 to 2 by using perturber ions of different masses. The authors have found an important effect in the central part of Hβ resulting in a smearing of the dip which becomes complete for $n_e \leq 2\times10^{15}$ cm^{-3}. Good agreement with a previous experiment at higher electron densities is observed. Furthermore, a narrowing of the peak separation of Hβ has been observed for the greatest ion velocities at electron densities lower than 5×10^{15} cm^{-3}. For Hα, the importance of the Doppler broadening would have required more accurate gas and ion temperatures, nevertheless an increase in the total width of the line is noted when the ion motion becomes faster.

I. INTRODUCTION

The 1973 experiments of Wiese *et al.*[1,2] (referred to as WKH hereafter) opened a great controversy over the effect of ion dynamics in the field of the Stark broadening of spectral lines. Later work has confirmed that a dynamical-ion effect actually existed in the central part of isolated lines,[3] as well as for quasidegenerate lines[4,5] and for degenerate lines.[6] On a theoretical plane for the hydrogen lines, several authors[7-11] have predicted such an effect. However, their approaches were rather different, and the detailed mechanism of the action of the ion motion in the line broadening process is still not understood.

For the Balmer lines, the main experimental work[2,6] in this field has been performed at electron densities greater than 10^{16} cm^{-3}. An extension of these measurements has become desirable, since in the first theoretical predictions[12] a measurable dynamical-ion effect was only expected at low electron densities ($n_e < 5\times10^{15}$ cm^{-3}). Therefore our purpose in the present work is to investigate the profiles of the lines Hα and Hβ of hydrogen in the electron density range 10^{15} cm^{-3} to 2×10^{16} cm^{-3}, and to study the ion motion effect in this area, which is still unexplored, as far as we know.

The experimental method used in this work was identical to the one used previously[4] for the line HeI 447.1 nm, and was based upon the variation of the reduced mass μ of the radiator–perturber-ion system as in the work by WKH. We have used a plasma jet created in a welding-type device, while other experiments were performed either in a wall-stabilized arc[2] or in a shock tube.[6] Thus the independence of the ion motion effects of the plasma-source type could be demonstrated. In this paper, we will describe the experimental and the plasma analysis methods and will present and discuss our results.

II. EXPERIMENTAL METHOD

A. Plasma source

The plasma device has been described previously.[4] It consists mainly of an improved conventional plasma jet with an excellent spatial stability. Four different plasma were studied, each one characterized by a different reduced mass of the radiator (hydrogen-atom)–perturbing-ion couple. The gas composition was adjusted in such a manner that in each plasma only one kind of ion was present or corresponded to more than 99% of the total number of ions. This was achieved by using mixtures of 0.1% of either H_2 or D_2 in Ar, in which case, we obtained $\mu_{H\text{-}Ar^+} = 0.975$ and $\mu_{D\text{-}Ar^+} = 1.9$, of 0.05% of H_2 in He with $\mu_{H\text{-}He^+} = 0.8$ and a mixture of 50% H_2 and 50% He, for which $\mu_{H\text{-}H^+} = 0.5$. In this last case, more than 99.9% of the ions came from hydrogen in our plasma conditions ($T_e \geq 10\,000$ K), and helium was used mainly to protect the electrodes from damages caused by the recombination of atomic hydrogen in molecular hydrogen. The major part of the excited atoms of helium are deexcited by collisions with a high energy-transfer rate; thus in the measurement area only the strongest lines of helium are observable.

The pressure in the plasma chamber varied from 100 to 300 torr. The electrical power, delivered by a stabilized rectifier, varied from 1.5 to 5 kW, and the gas flow, at atmospheric pres-

sure, varied from 80 to 250 cm^3/s. Various combinations of these quantities allowed electron density changes from 10^{15} up to 2×10^{16} cm^{-3}. The lines Hα and Hβ or similarly Dα and Dβ, were easily observable in each case.

The cylindrical symmetry of the jet required side-on observation and the use of the Abel inversion process. Therefore, for each line, 15–25 profiles were recorded at different positions of the jet across the entrance slit of the spectrometer. A great number of measurements required a rather long working time, more than three hours for each experiment; thus the stability was continuously checked by measuring the total intensity of the line Hα. Deviations were always lower than 2% of the total intensity. Great care was taken in the Abel inversion procedure in order to limit errors. Symmetry was checked by comparing the profiles measured on both sides of the jet, and the radius was determined by a careful investigation of the plasma edges. Finally, the Abel inversion was performed by means of an extremely accurate program[13] rearranged for microcomputer use.

B. Optical setup

A schematic description of the optical setup is given in Fig. 1. The spectrometer has a 1200-lines/mm grating and a focal length of 1.70 m, allowing a reciprocal dispersion of 0.44 nm/mm in the first order at $\lambda = 486.1$ nm. This dispersion could grow up to 0.055 nm/mm in the third order at this wavelength. The slit width was fixed at 5 μm; thus the spectral resolution was entirely given by the optical multichannel analyzer (OMA) which served to measure the line profiles.

The sensitive head of the OMA was formed by a plate divided into 500 contiguous channels, each having a width of 25 μm and a height of 5 mm.

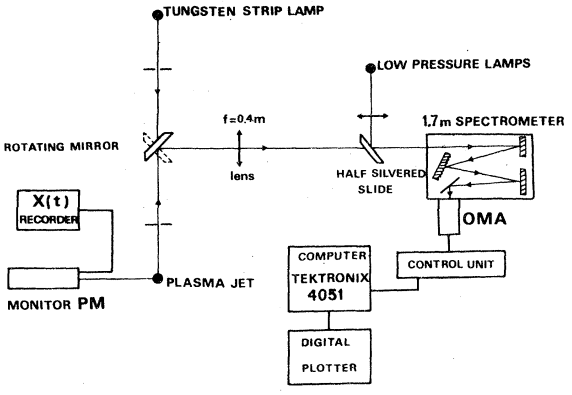

FIG. 1. Schematic diagram of the optical experimental setup. OMA: optical multichannel analyzer, PM: photomultiplier.

This plate was set in the focal plane of the spectrometer. Measurements have shown that the apparatus width (at e^{-1}) was about three channels broad whatever the wavelength and the order of dispersion might be. This was caused by the light diffusion between neighboring channels inherent to the OMA construction. Thus the functional half-width of the apparatus was about 0.025 nm in the first order and about 0.0032 nm in the third order for $\lambda = 486.1$ nm. The energy response of the OMA was checked by means of a calibrated tungsten ribbon lamp at each measured wavelength channel by channel. Variations in the channel responses of about 35% were found from the edge (channel 0) to the center (channel 250) of the plate. This procedure permitted a direct measurement of the absolute line intensities. The main advantage in using OMA resulted from the possibility of numerous summations of the luminous signal over short periods of time. Typically, 1000 summations over 30 s were realized. Thus a considerable improvement of the signal-to-noise ratio was obtained. Finally the OMA was coupled to a minicomputer, allowing rapid storage of the digitalized data on magnetic tapes, followed by the processing of the data.

C. Measurement of line profiles

For numerous lines the continuous background under the line was negligible. In other cases, such as Hβ in an argon plasma, the background, due mainly to argon, was determined in a pure argon plasma, operated under the same conditions. Thus by comparison it was possible to separate the hydrogen and the argon contributions in the observed spectra.

The line wings of Hα and Hβ were estimated by the asymptotic formula given by Kepple and Griem (KG).[14] The error in the line area determination was finally estimated to be about 1–3% for Hβ and 4 or 5% for Hα. The lines of Ar II, which were superimposed on the line Hβ, were easily eliminated, owing to the good spectral resolution of our apparatus. Moreover, the region of interest, i.e., the line center, was not perturbed by such lines.

In another way, the only unidentified lines observed in our experiments were probably lines of H_2 but with intensities of about 10^{-5} times the total intensity of Hα or Hβ, while the observed effects (see Fig. 5, for instance) represented about 10^{-2} or more of the total line intensity.

D. Other broadening mechanisms

Under our experimental conditions, $T_e \gtrsim 10\,000$ K and $n_e \gtrsim 10^{15}$ cm^{-3}, the pressure effect was negligible for all observed lines of Ar I, He I, or H I.

The Doppler effect might be considered at least for the lowest electron densities in the line profiles and, for a number of lines, it became the main broadening process. For instance, the Doppler width of Hα was 0.047 nm at $T = 10\,000$ K, while at $n_e = 2\times 10^{15}$ cm^{-3}, the total width was only about 0.1 nm, depending on the reduced mass. For the line Hβ, the thermal motion induced only a correction consisting of a smearing of the central structure of the line (Fig. 3). Nevertheless, as shown in Fig. 3, this effect alone could not explain the actual observed profiles. The influence of the self-absorption was calculated from the ratio of the line intensity $I(\lambda)$ multiplied by the effective length of the plasma d_{eff}, to the blackbody intensity at the plasma temperature $B_0(\lambda, T)$, then using the relation

$$I(\lambda)d_{\text{eff}} = B(\lambda, T)\left[1 - \exp\left(-\int k(\lambda)dx\right)\right];$$

$k(\lambda)$ being the absorption coefficient. We then obtained

$$\tau = \int k(\lambda)dx \simeq k(\lambda)d_{\text{eff}},$$

where τ is the optical depth. Even in the (nearly) pure hydrogen plasma, with $d_{\text{eff}} \geq 3$ mm, the maximum value of τ for Hα was only 3×10^{-2}. In every other case, the value of τ became smaller than 10^{-4}. Thus we could neglect the influence of self-absorption in the line profiles.

III. PLASMA ANALYSIS

A determination of the gas temperature T_g was required in order to calculate the influence of the thermal motion in line profiles; moreover, under the realistic assumption that $T_g = T_i$ this measurement would also give the ion temperature T_i, which was of great interest in the present study. These temperatures were obtained from the measurements of the Doppler widths of some isolated lines of ArI or HeI, for which the Stark effect has the weakest possible influence. Unfortunately, in the observable spectral range, from 250 to 850 nm, the Stark effect was never entirely negligible, at least for $n_e \geq 5\times 10^{15}$ cm^{-3}, for the isolated lines of the plasma. A deconvolution process was then involved, in which the apparatus function was also taken into account. The uncertainties in the theoretical Stark widths of the isolated lines were about 20–30%, but they could induce errors exceeding 40% in the Doppler widths after the deconvolution process. In turn, the gas temperature showed uncertainties up to 80%. However, for the lowest electron densities the Stark effect was almost negligible for the selected lines, and the error in the determination of T_g decreased to about 20%. At these low densities, the line Hα could be used in the gas temperature determination with the HeI isolated lines. The values obtained from Hα were in very good agreement with those given by the HeI lines. We found that, except in He plasmas, T_g or T_i did not differ by much (10%) from the electron temperature T_e. For helium plasmas, a systematic discrepancy was found which indicated a gas temperature about 3000 K lower than T_e. Subsequently, for the greatest densities it was assumed that the same features were also available. It is worth noting at this point that if T_i or T_g occur in the line profiles only by their square roots, either by the Doppler broadening or by the ion-velocity effect, then the importance of errors is significantly decreased. The electron density was easily deduced from the Hβ profile by comparison with the theoretical profiles from KG. Except in the line center, and also for the lowest electron densities, excellent agreement was observed. The uncertainties could be estimated to be about 10% for $n_e \geq 5\times 10^{15}$ cm^{-3}, but they could increase up to 20% at 10^{15} cm^{-3}.

The electron temperature T_e has generally a small influence in the Stark broadening. Nevertheless, the accuracy attained in the line-profile determination was such that every parameter having an influence on this profile should be known as accurately as possible. Two methods using the intensities of lines arising from levels in partial thermodynamic equilibrium were used in the determination of T_e, first by the ratio of line intensities and secondly by use of the Saha equations. Another method using the collisional-radiative model[15,16] was applied to the plasma. In this case, the plasma was considered as stationary and the diffusion, mainly of the atoms in ground state, was neglected. This model, used in connection with the equations of state, of neutrality, of Saha, and with the initial chemical composition of the plasma, enabled us to determine the plasma composition as well as the electron temperature. The temperatures obtained from the three different methods were in reasonable agreement with deviations of about 10% except for the (nearly) pure helium plasma where the divergences could exceed 25%. In this last case the diffusion of the atoms in ground state could likely explain the calculated discrepancies.

Finally, the electron temperatures varied from about 9000 up to 14 000 K for the argon or hydrogen plasmas with the reduced masses $\mu = 0.5$, 0.975, and 1.9, and from 12 500 up to 20 000 K for the helium plasmas with small admixtures of hydrogen ($\mu = 0.8$). Thus the ion temperatures were in

the ranges 9000–17 000 K and 9000–14 000 K without the helium plasma as in Fig. 6 for example.

IV. RESULTS AND DISCUSSION

A. Hβ

The variation of the peak separation S (in nm) is shown in Fig. 2 as a function of n_e for the four different reduced masses. The theoretical values from KG are also reported. If we take into account the experimental uncertainties indicated in the figure, we may report good agreement between theory and experiment for $n_e > 6\times 10^{15}$ cm^{-3}, thus confirming numerous previous studies for equal or higher electron densities. On the other hand, discrepancies appear for the lowest electron densities, especially for $\mu = 0.5$. We find that S decreases with the reduced mass μ at a constant electron density, although the differences between the reported values for $\mu = 0.8$, 1, and 1.9 are within experimental error except at the lowest electron densities. However, the results of several experiments are well superimposed on each other for the same μ. In this figure the main error arises from the electron density measurement and is about 20%, while the error in the measurement of S is smaller than 10%; furthermore the relative error in electron density between the profiles for different reduced masses is well below 20% because these profiles have about the same half-widths. Apart from such physical explanations as modifications in the probability distribution of the ion microfield caused by ion motion, we have been unable to see what kind of phenomenon could account for this narrowing of the peak separation. More particularly, the plasma inhomogeneities were first taken into account by means of the Abel inversion; moreover the inhomogeneity was rather weaker in the case $\mu = 0.5$, with the narrowest S, than for the other reduced masses; second, the self-absorption of the line Hβ was completely negligible, the calculated optical thickness being less than 4×10^{-4}; and third, the influence of the Doppler effect on S seems negligible, as shown in Fig. 3. This figure shows that the narrowing of S is closely related to the dip smearing of the line. We note that the line core, between about −0.1 and 0.1 nm, is not as well fitted by the theory as at higher electron densities (Fig. 5), while the experimental wings ($|\Delta\lambda| \geq 0.2$ nm) lie slightly above the theoretical ones. These discrepancies from the theory observable up to 5×10^{15} cm^{-3} are responsible for the important uncertainties in the determination of the lowest electron densities. An examination of the literature shows a similar effect[17] at $n_e = 10^{15}$ cm^{-3}, $T_e \simeq 10\,000$ K and $\mu = 0.5$, while for $\mu = 0.8$ (Ref. 17) or 1 (Ref. 18), the narrowing of the peak separation is almost negligible. The most remarkable feature which appears in Fig. 3 is the smearing of the central structure of the line; it is completely eclipsed for $\mu = 0.5$, while there is still a trace of a dip for $\mu = 0.8$. The variation of the dip factor D, defined as

$$D = (I_{max} - I_{min})/I_{max},$$

as a function of the electron density is plotted in Fig. 4 (I_{max} and I_{min} are defined in Fig. 3). Three features appear in this figure. First, the influence of the ion motion on the dip factor is clearly demonstrated by the wide differences between the curves corresponding at different reduced masses; second, a rather good agreement exists, for $n_e \simeq 2\times 10^{16}$ cm^{-3}, with the WKH results, reported in this figure, for each reduced mass; third, the dip is completely smeared out at low electron densities, as stated above in Fig.

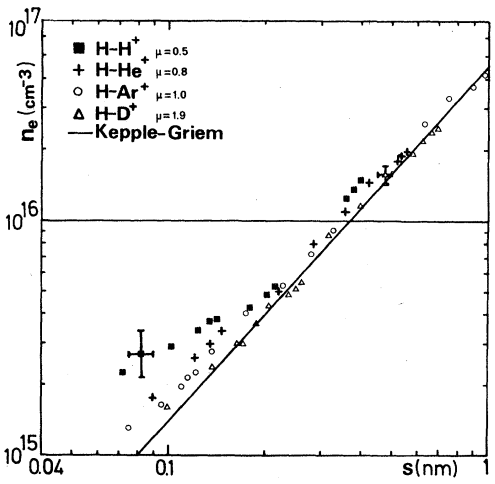

FIG. 2. Variation of the peak separation S of Hβ vs electron density, for the different reduced masses.

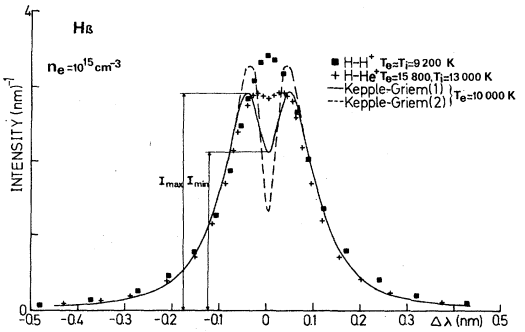

FIG. 3. Profiles of Hβ, normalized in area, at about $n_e \simeq 10^{15}$ cm^{-3}. Theoretical profiles by KG convolved with Doppler profile (1) and without convolution (2).

3, and it disappears gradually from about 2×10^{15} cm^{-3} for $\mu=0.5$ to 10^{15} cm^{-3} and lower for $\mu=1.9$. The theoretical curve tends also towards zero for small electron densities, but only under the influence of the Doppler effect, while otherwise, without this thermal effect, the theoretical dip factor tends towards 1. The dependence of the dip intensity on the reduced mass is shown in Fig. 5 at an electron density $n_e \simeq 5\times10^{15}$ cm^{-3}, in which the profiles of Hβ, normalized in area, are in excellent agreement with the theory for the different reduced masses, except in the central part from about −0.2 to 0.2 nm. No mechanism other than an ion-motion effect can entirely explain the observed variations of the Hβ profiles with the reduced mass, because first, the electron and the ion temperatures reported in Fig. 5 are nearly the same as in every other case with different electron density; thus the Doppler effect is of comparable importance for each line. Secondly, the agreement between theory and experiment can be increased by the inclusion in the calculations of the time-ordering operator[19] or of the inelastic collisions for the electron collision operator,[20] but these corrections are independent of the reduced mass, and they cannot account, alone, for the observed effects.

Finally, we have plotted in Fig. 6 the dip factor versus $\mu^{-1/2}$, this quantity being proportional to the ion velocity, for several electron densities. In contradiction with the WKH results for $n_e \geq 2\times10^{16}$ cm^{-3}, our experimental points, extracted from the averaged curves in Fig. 4, are not on a straight line; however, an extrapolation of these curves (dashed lines) at an infinite reduced mass, i.e., $\mu^{-1/2}=0$, suggests that a good convergence exists between the static theory of KG and our experiment with very low ion temperatures. To be consistent, however, we may note that, for $n_e=10^{16}$ cm^{-3}, only a slight modification of the averaged experimental points, within experimental error, would allow a linear variation of D with $\mu^{-1/2}$, as observed by WKH. Finally, as the ion temperatures are about the same for each electron density, the variation of D with $(T_i/\mu)^{1/2}$ would show curves identical to the one in Fig. 6.

On a theoretical plane, some work predicts a modification of the central part of the line, as in the experiment, but discrepancies still exist. For instance, Lee[21] and Cooper *et al.*[11] do not find a total smearing of the dip at $n_e=10^{15}$ cm^{-3} and $T_e=10^4$ K as in the present work that by Burgess and Mahon[17] for $\mu=0.5$. At higher electron density, Seidel[7] finds important dynamical corrections, but his results for $\mu=0.5$ are in poor agreement with the experimental values (Fig. 4). Demura *et al.*[22] predict theoretically a variation of the dip as a linear function of μ^{-1} and $n_e^{-4/3}$, and they find a relatively good linear interpolation of the WKH results; in the present work, the variation of the dip as a function of μ^{-1} would not show a linear variation, but, as in Fig. 6, minor changes in the experimental points, within experimental error, would give this linear variation of the dip factor with μ^{-1}. Recently, Sholin[23] has corrected the calculations by Demura *et al.*[22] and finds a variation of the dip intensity scaling as $\mu^{-1/2}n_e^{-1/3}$.

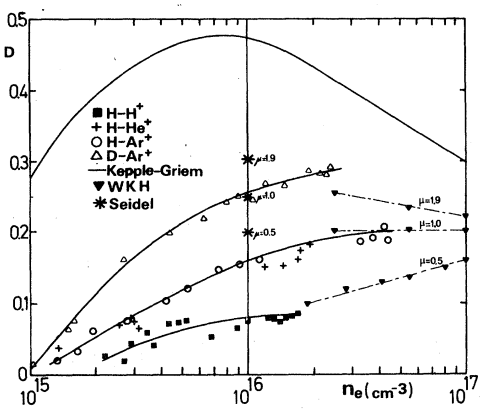

FIG. 4. Variation of the dip factor D of Hβ vs electron density for different reduced masses. Comparison with the static theory of KG, including a convolution with the Doppler profile. The theoretical points of Seidel at $n_e=10^{16}$ cm^{-3} take the ion motion into account but do not include the Doppler effect. The experimental points by WKH are also reported.

B. Hα

For this line, the Doppler effect becomes predominant for an electron density of about 3×10^{15} cm^{-3}, and it gives an important contribution to

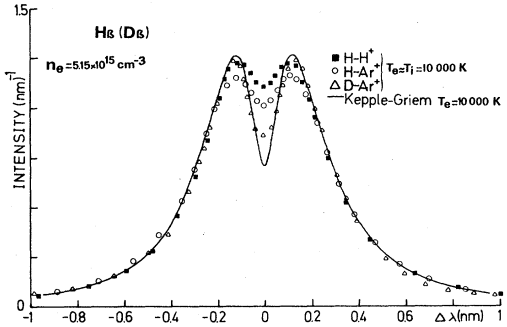

FIG. 5. Profiles of Hβ normalized in area, at $n_e \simeq 5.15\times10^{15}$ cm^{-3}, showing the smearing of the central dip for the different reduced masses and for the static theory by KG. No measurable asymmetry was noted in the experimental peaks.

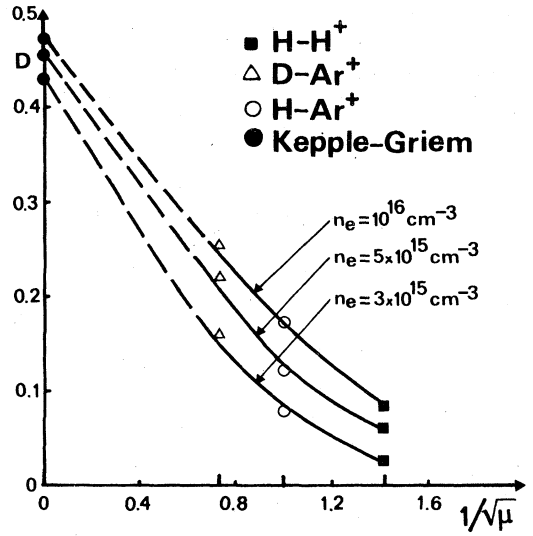

FIG. 6. Variation of the dip factor D of Hβ vs $\mu^{-1/2}$. The experimental points are extracted from Fig. 4. The dashed lines represent an attempt in the extrapolation of the experimental values at an infinite reduced mass.

the profile up to 10^{16} cm^{-3}. Thus highly accurate temperatures are required in order to compare the different profiles. Furthermore, several difficulties arise in the determination of line profiles: first, the wing contribution to the total area of the line is important, and, although the background continuum was of little importance, the uncertainty in the line-wing determination can cause errors of about 3–5% in the total intensity of the line. With the addition of the experimental errors of about the same amplitude and some self-absorption effects (less than 2% in case of the pure hydrogen plasma) the total amount of error in the profile determination can go beyond 10%. This quantity is of the order of the discrepancy amplitude observed in our experiment between each profile at different reduced masses. Nevertheless, as shown in Figs. 7 and

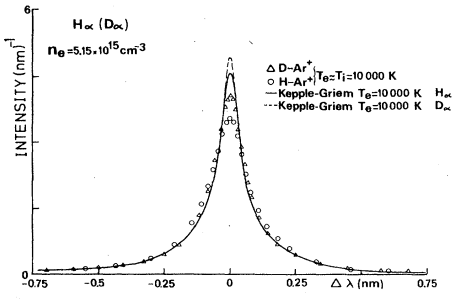

FIG. 7. Profiles of Hα at $n_e \simeq 5.15\times10^{15}$ cm^{-3} for two reduced masses and for the static theory of KG convolved by the Doppler profile for hydrogen (1) and deuterium (2).

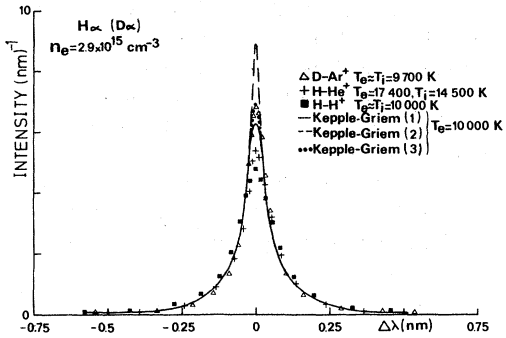

FIG. 8. Profiles of Hα at $n_e \simeq 2.9\times10^{15}$ cm^{-3} for different reduced masses. Theoretical profiles by KG convolved with Doppler profile for hydrogen (1), for deuterium (3), and without convolution (2).

8, we have found an ion-motion effect which increases the total width of the line, or, in a related manner, decreases the central peak intensity. In these figures a better agreement exists between theory and experiment for $\mu = 1.9$ than for $\mu = 1$ or 0.5. In Fig. 8, the profile at $\mu = 1.9$, i.e., the line Dα, is in good agreement with the theory convolved with the Doppler effect for deuterium. We note the great influence of the Doppler broadening in this case, and then the need for an extremely accurate temperature determination.

V. CONCLUSION

The results reported in this paper corroborate and complete those previously obtained at higher electron densities by other authors. As expected, the effect of ion motion on the lines Hα and Hβ is important at low electron densities; however, as shown in Fig. 4, this effect is attenuated towards 10^{15} cm^{-3}. This is due mainly to thermal motion, which tends to mask the ion-velocity effect. We have noted a total smearing of the central structure of Hβ for about 10^{15} cm^{-3}, depending on the reduced masses; nevertheless, we can assume, following Fig. 6, that for much lower ion temperatures than ours ($T_i < 10\,000$ K) the dip will always exist for densities well below 10^{15} cm^{-3}, as indicated by the static theory. Another unexpected aspect of the ion-motion effect is the narrowing of the peak separation for $n_e \leq 5.10^{15}$ cm^{-3}, especially for hydrogen-ion perturbers, i.e., $\mu = 0.5$. No error of such importance could be detected in our measurements; thus it can be suggested that there perhaps exists a modification in the ion microfield distribution, caused by the ion motion, inducing a shift in the Stark-component positions. For the time being, Hey and Griem[24] and, in a more elaborate manner, Demura

et al.,[22] have used a modified distribution for the ion microfield including the ion motion, but no prediction of such an effect is reported in these papers. Thus the problem is still open.

In conclusion, it would be very interesting to get some measurements of Hα or Hβ profiles in plasmas having very low ion temperature in order to check the validity of the extrapolation in Fig. 6 between finite and infinite reduced masses.

Finally, it seems necessary to determine the electron density from independent measurements not involving the line broadening, at least for densities below 5×10^{15} cm^{-3}.

ACKNOWLEDGMENT

We acknowledge Mr. G. Grenier, who had an important role in the plasma arc operation.

[1]D. E. Kelleher and W. L. Wiese, Phys. Rev. Lett. 31, 1431 (1973).
[2]W. L. Wiese, D. E. Kelleher, and V. Helbig, Phys. Rev. A 11, 1854 (1975).
[3]D. E. Kelleher, Technical Note BN-865, Institute for Science and Technology, University of Maryland, 1978 (unpublished).
[4]C. Fleurier, G. Coulaud, and J. Chapelle, Phys. Rev. A 18, 575 (1978).
[5]H. Ehrich and V. Helbig (unpublished).
[6]J. L. Chotin, J. L. Lemaire, J. P. Marque, and F. Rostas, J. Phys. B 11, 371 (1978).
[7]J. Seidel, Z. Naturforsch. A 32, 1207 (1977).
[8]V. S. Lisitsa, Usp. Fiz. Nauk 122, 445 (1977) [Sov. Phys. Usp. 20, 603 (1977)].
[9]R. W. Lee, J. Phys. B 11, L167 (1978).
[10]R. W. Lee, J. Phys. B 12, 1445 (1979).
[11]J. Cooper, E. W. Smith, and C. R. Vidal, J. Phys. B 7, L101 (1974).
[12]D. D. Burgess, J. Phys. B 3, L67 (1970).
[13]C. Fleurier and J. Chapelle, Comput. Phys. Commun. 7, 200 (1974).
[14]P. Kepple and H. R. Griem, Phys. Rev. 173, 317 (1968).
[15]H. W. Drawin and F. Emard, Report EUR-CEA-FC 697, Association Euratom CEA (Fontenay-aux-Roses), 1972 (unpublished).
[16]K. Katsonis, thesis, University of Paris-Sud, 1976 (unpublished).
[17]D. D. Burgess and R. Mahon, J. Phys. B 5, 1756 (1972).
[18]D. L. Evans, D. D. Aeschliman, and R. A. Hill, Phys. Rev. A 6, 2430 (1974).
[19]L. J. Roszman, Phys. Rev. Lett. 31, 785 (1975).
[20]R. A. Hill, J. B. Gerardo, and P. C. Kepple, Phys. Rev. A 3, 855 (1971).
[21]R. W. Lee, J. Phys. B 6, 1060 (1973).
[22]A. V. Demura, V. S. Lisitsa, and G. V. Sholin, Zh. Eksp. Fiz. 73, 400 (1977).
[23]G. V. Sholin, in Proceedings of the Fourteenth International Conference on Phenomena in Ionized Gases, Grenoble, 1979 (unpublished).
[24]J. D. Hey and H. R. Griem, Phys. Rev. A 12, 169 (1975).